Supporting information

Achieving increased resolution and reconstructed image quality with gradient variance modified super-resolution radial fluctuations

Xingyu Gong [1,5], Li Zhou [2,5], Longfang Yao [1], Li Zhang [2], Liwen Chen [1], Yiyan Fei [1], Lan Mi [1,*], Baoju Wang [3,*] and Jiong Ma [1,2,4,*]

[1] Department of Optical Science and Engineering, Shanghai Engineering Research Center of Ultra-precision Optical Manufacturing, Key Laboratory of Micro and Nano Photonic Structures (Ministry of Education), Green Photoelectron Platform, Fudan University, 220 Handan Road, Shanghai 200433, China.

[2] Shanghai Engineering Research Center of Industrial Microorganisms, The Multiscale Research Institute of Complex Systems (MRICS), School of Life Sciences, Fudan University, 220 Handan Road, Shanghai 200433, China

[3] Centre for Optical and Electromagnetic Research, Guangdong Provincial Key Laboratory of Optical Information Materials and Technology, South China Academy of Advanced Optoelectronics, South China Normal University, Guangzhou 510006, China.

[4] Institute of Biomedical Engineering and Technology, Academy for Engineer and Technology, Fudan University, 220 Handan Road, Shanghai 200433, China

[5] These authors contributed equally: Xingyu Gong and Li Zhou

[*] email: lanmi@fudan.edu.cn; baoju.wang@m.scnu.edu.cn; jiongma@fudan.edu.cn

1. Theoretical distinguishable distance of double blinking fluorophores.

In general, the resolution of fluorescence imaging is defined by the full width at half maximum (FWHM) of a point spread function (PSF). The diffraction limit of optical microscope is described as $d = \lambda/(2\mathrm{NA})$, where λ is the wavelength and NA the numerical aperture of the microscope[1]. The theoretical limit is approximately half of the wavelength with NA equal to 1, and smaller with commonly higher NA in most advanced fluorescence microscope. While, in the discussion of weighting function, the resolution, which is also the FWHM of PSF, is 200 nm (λ = 580 nm, NA=1.45) in widefield imaging. For a Gaussian PSF, its FWHM is equal to $2\sqrt{2\ln 2}\sigma$, where σ is the standard deviation of the Gaussian function.

Assume that there are two blinking fluorophores (Fig. S1a) described by [$\mathbf{r}_1(d/2,0)$, a_1, $f_1(t)$] and [$\mathbf{r}_2(-d/2,0)$, a_2, $f_2(t)$]. Let $a_1 = a_2$, $D[f_1(t)] = D[f_2(t)]$. W_p and W_m are the value of $W(\mathbf{r})$ at the center of one molecule and at midpoint of the line segment between the two fluorophores respectively. It is easily derived:

$$W_p = \frac{1+U(d)^2}{d^2U(d)^2},\ W_m = \frac{4}{d^2}. \tag{1}$$

Define a relative concave margin as a function of d: $M(d) = (W_p - W_m)/W_m$. Obviously, $M(d)>0$ is meaningful to distinguish two peaks of the PSFs. The gradient vector field at midpoint become outwards instead of inwards when $M(d)>0$. Though the change is inappreciable in terms of intensity, it is still a significant transformation of degree of local gradient convergence for SRRF to detect. The critical value d_{th} can be calculated in condition that $W_p = W_m$, which is $\sqrt{\ln 3}\sigma$ or $0.5\sqrt{0.5\log_2 3}$ FWHM. Finally, the theorotical critical distinguishable distance of double blinking fluorophores is demonstrated. The relative concave margin curves of intensity variance and intensity average are also ploted and the corresponding critical distances are shown in Fig. S1b.

2. Errors of measured distance of double-lines.

In the simulation of double-lines, the measured distance of double-lines in gmSRRF image tend to be a little smaller than true distance. As shown in Fig. S1c, the average of measured distances was approximately 84.6 nm, a 6% less than presupposed 90 nm. Actually, peaks of $W(\mathbf{r})$ exhibit a shift towards center as the central intensity increases. Therefore, as the double-lines become closer, $W(\mathrm{r})$ is less functional to split the overlapping PSFs completely by the real distance.

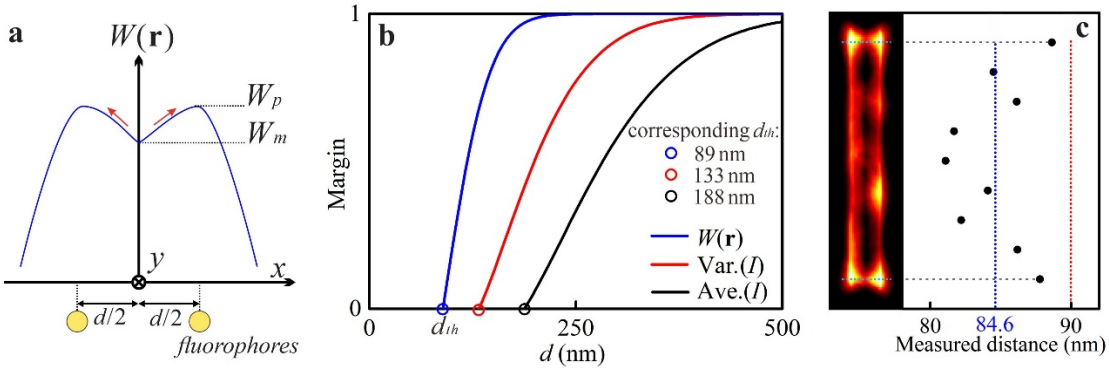

Fig. S1 a Schematic diagram of $W(\mathbf{r})$ curve in vertical section parallel to x axis. The relative sizes of W_p and W_m determine whether the local gradient field (red arrows) between the two fluorophores orients outwards or inwards. **b** Concave margin curves as a function of d. M(d) =0 defines the critical distances. **c** Left: gmSRRF image of 90 nm double-lines in Fig. 2d; right: measured distances corresponding to the horizontal positions of double-lines. Blue dot line indicates the average of measured distances (84.6 nm).

3. Comparison with deconvolution.

The gmSRRF algorithm determines likelihood of real PSF centers by extracting time-varying properties from fluorescence fluctuations. And when it comes to restoring ground-truth object, deconvolution algorithms play an important role. It's valuable to discuss which of deconvolution and weighting function performs better in modifying raw sequence and supporting SRRF. Therefore, we introduced Richardson-Lucy deconvolution[2, 3] (MATLAB R2020a, 'deconvlucy' function) to all the raw data mentioned in experimental section before processing them with SRRF. Some typical regions focused on resolution and artifacts are shown in Fig. S2. Although the deconvolution algorithms could also play a slight role in the aspect of reducing reconstructed SRRF images artifacts, the gmSRRF algorithm was more effective, especially in removing noise and reconstructed artifacts, as shown in Figs. S2b-f.

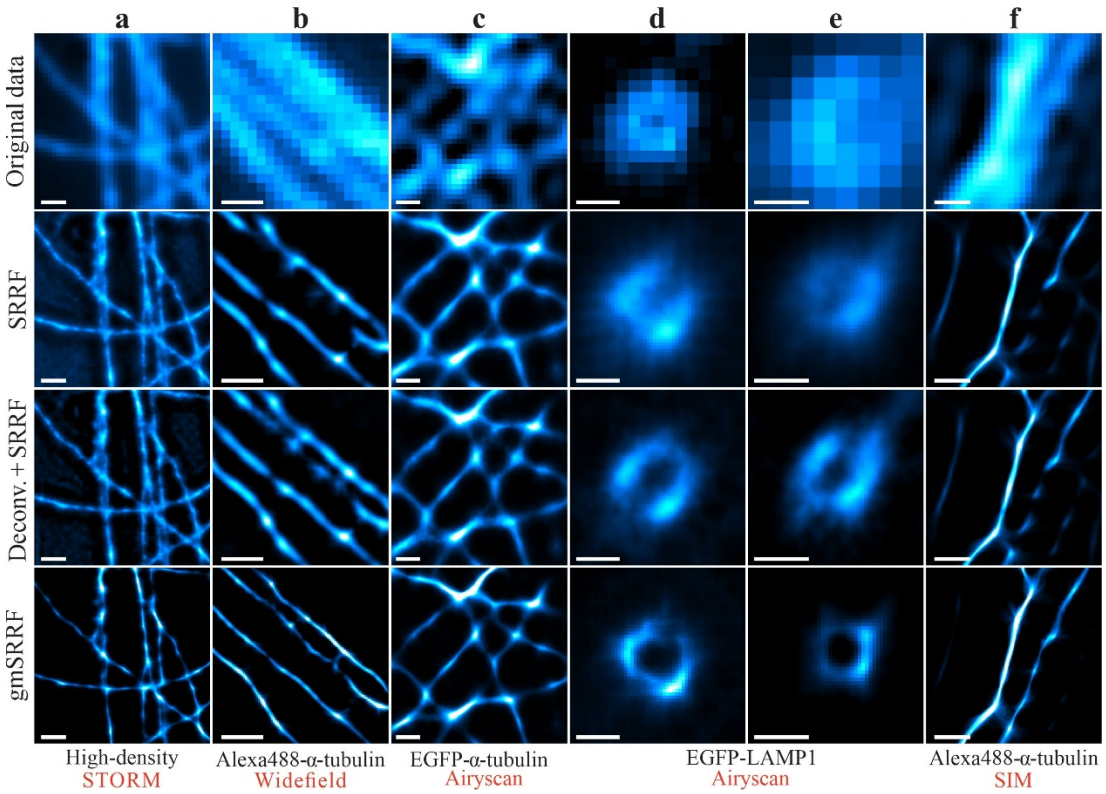

Fig. S2 a-f Columns: high density STORM image, widefield image of microtubules, Airyscan of microtubules, lysosomes, and SIM image of microtubules. Reconstructed images restored by deconvolution and post-processed with SRRF were inserted to the canvas and compared with the gmSRRF algorithm. **a-b** Column scale bars: 500 nm. **c-f** Column scale bars: 200 nm.

4. Images acquisition information

Table1 Acquisition parameters of experimental images

Iterms	Number of frames	Exposure time/frame (ms/fps)
high-density STORM	500	40
widefield microtubules	500	20
Airyscan microtubules	100	1476
Airyscan lysosomes	250	412
SIM *trans*-Golgi	200	90
SIM microtubules	70	100

References

1. Abbe, E. Beiträge zur Theorie des Mikroskops und der mikroskopischen Wahrnehmung. *Archiv für Mikroskopische Anatomie* **9** (1), 413-468 (1873). 10.1007/BF02956173
2. Richardson, W. H. Bayesian-Based Iterative Method of Image Restoration. *J. Opt. Soc. Am.* **62**

(1), 55-59 (1972). Doi 10.1364/Josa.62.000055

3. Fish, D. A., Walker, J. G., Brinicombe, A. M. & Pike, E. R. Blind deconvolution by means of the Richardson–Lucy algorithm. *J. Opt. Soc. Am. A* **12** (1) (1995). 10.1364/josaa.12.000058